**RESEARCH ARTICLE** | *Cellular and Molecular Properties of Neurons*

# Nucleus accumbens core medium spiny neuron electrophysiological properties and partner preference behavior in the adult male prairie vole, *Microtus ochrogaster*

Jaime A. Willett,[1,2,3] Ashlyn G. Johnson,[1,2] Andrea R. Vogel,[1,2,4] Heather B. Patisaul,[1,2,5] Lisa A. McGraw,[1,2,4] and John Meitzen[1,2,5,6]

[1]Department of Biological Sciences, North Carolina State University, Raleigh, North Carolina; [2]W. M. Keck Center for Behavioral Biology, North Carolina State University, Raleigh, North Carolina; [3]Graduate Program in Physiology, North Carolina State University, Raleigh, North Carolina; [4]Graduate Program in Genetics, North Carolina State University, Raleigh, North Carolina; [5]Center for Human Health and the Environment, North Carolina State University, Raleigh, North Carolina; and [6]Comparative Medicine Institute, North Carolina State University, Raleigh, North Carolina

Willett JA, Johnson AG, Vogel AR, Patisaul HB, McGraw LA, Meitzen J. Nucleus accumbens core medium spiny neuron electrophysiological properties and partner preference behavior in the adult male prairie vole, *Microtus ochrogaster*. *J Neurophysiol* 119: 1576–1588, 2018. First published January 17, 2018; doi:10.1152/jn.00737.2017.—Medium spiny neurons (MSNs) in the nucleus accumbens have long been implicated in the neurobiological mechanisms that underlie numerous social and motivated behaviors as studied in rodents such as rats. Recently, the prairie vole has emerged as an important model animal for studying social behaviors, particularly regarding monogamy because of its ability to form pair bonds. However, to our knowledge, no study has assessed intrinsic vole MSN electrophysiological properties or tested how these properties vary with the strength of the pair bond between partnered voles. Here we performed whole cell patch-clamp recordings of MSNs in acute brain slices of the nucleus accumbens core (NAc) of adult male voles exhibiting strong and weak preferences for their respective partnered females. We first document vole MSN electrophysiological properties and provide comparison to rat MSNs. Vole MSNs demonstrated many canonical electrophysiological attributes shared across species but exhibited notable differences in excitability compared with rat MSNs. Second, we assessed male vole partner preference behavior and tested whether MSN electrophysiological properties varied with partner preference strength. Male vole partner preference showed extensive variability. We found that decreases in miniature excitatory postsynaptic current amplitude and the slope of the evoked action potential firing rate to depolarizing current injection weakly associated with increased preference for the partnered female. This suggests that excitatory synaptic strength and neuronal excitability may be decreased in MSNs in males exhibiting stronger preference for a partnered female. Overall, these data provide extensive documentation of MSN electrophysiological characteristics and their relationship to social behavior in the prairie vole.

**NEW & NOTEWORTHY** This research represents the first assessment of prairie vole nucleus accumbens core medium spiny neuron intrinsic electrophysiological properties and probes the relationship between cellular excitability and social behavior.

Address for reprint requests and other correspondence: J. A. Willett, Dept. of Biological Sciences, NC State Univ., Campus Box 7617, 144 David Clark Labs, Raleigh, NC 27695-7617 (e-mail: jawillet@ncsu.edu).

electrophysiology; medium spiny neuron; nucleus accumbens; rat; vole

## INTRODUCTION

The prairie vole (*Microtus ochrogaster*) has emerged as a key model animal for studying social behavior (Hammock and Young 2006; McGraw and Young 2010; Young et al. 2011) because strong pair bonds form between males and females that persist in multiple breeding cycles (Carter and Getz 1993; Young et al. 2011). Social monogamy and preference for the bonded partner animal occur in <5% of mammals (Kleiman 1977) and even fewer laboratory-tractable rodents. Thus the prairie vole has enabled significant advances in elucidating the underlying neurobiological and genetic mechanisms for these and other prosocial behaviors (Aragona et al. 2006; Bosch et al. 2009; Carter et al. 1995; Lim et al. 2004).

Prairie voles are remarkable in that they display significant individual variation within the unique social behaviors they exhibit (Barrett et al. 2013; Perkeybile et al. 2013), including partner preference (Hammock and Young 2005). This variability in vole social behavior is mirrored by variability in the underlying neural substrate, with the role of social neuropeptides such as vasopressin and oxytocin being exceptionally well explored. For example, resident male space use and sexual fidelity are positively correlated with vasopressin receptor density at the retrosplenial cortex (Okhovat et al. 2015; Ophir et al. 2008). In female voles, oxytocin receptor density in the nucleus accumbens is positively associated with individual and species variation in alloparental and other social behaviors (Insel and Shapiro 1992; Olazábal and Young 2006a, 2006b; Ross et al. 2009). This individual variation in social neuropeptide density and behaviors predicts that the brain regions involved with these behaviors should likewise show variation in their cellular properties, electrophysiological and/or anatomical.

Multiple neural loci have been implicated in partner preference behaviors, including the nucleus accumbens (Aragona et al. 2003, 2006). Part of the striatum, the nucleus accumbens is a nexus region that plays a prominent role in controlling social, motivated, and reward behaviors related to both natural and pathological reinforcers, select motivational and emotional processes, and mood disorders (Salgado and Kaplitt 2015; Yager et al. 2015) and is necessary for pair bond formation and maintenance (Aragona et al. 2003, 2006). The nucleus accumbens is currently subdivided into two subregions: the core (NAc) and the shell, which show differential functions and anatomical projections.

Here we targeted the NAc, which receives multiple glutamatergic inputs from the hippocampus, amygdala, prefrontal cortex, and thalamus in addition to dopaminergic and GABAergic inputs (Groenewegen et al. 1999; Kelley 2004). The numerous inputs to the NAc are synthesized into output by the GABAergic medium spiny neurons (MSNs), which comprise ~95% of the neuron population and project outside of the NAc to directly influence motor and cognitive behaviors (Smith et al. 2013; Yager et al. 2015). There are a number of intrinsic electrophysiological properties that determine an MSN's response to input. Prominent among these is membrane excitability, a property predicated on the neuron's ion channel composition, which determines the likelihood that the neuron will produce an action potential in response to stimulation. Increased excitability translates to heightened responsivity to excitatory input, and changes in MSN excitability directly relate to changes in behavior (Grillner et al. 2005; Mu et al. 2010; Tan et al. 2013). To our knowledge, no study has ever characterized vole MSN intrinsic electrophysiological properties beyond local field potentials and optogenetically stimulated excitatory postsynaptic currents (Amadei et al. 2017). Furthermore, no study has tested how these intrinsic properties vary with the strength of the pair bond between partnered voles.

To determine the relationship between intrinsic electrophysiological properties and pair bond strength, we performed whole cell patch-clamp recordings of MSNs in acute brain slices of the NAc of adult male voles exhibiting strong and weak preferences for their respective partnered females. To provide essential context for MSN electrophysiological properties, we also performed recordings of MSNs in acute brain slices of the NAc of adult male rats. We then extensively compared vole and rat MSN electrophysiological properties, including action potentials, excitability, passive and input resistance properties, and miniature excitatory postsynaptic current (mEPSC) properties. Vole MSNs demonstrated many canonical electrophysiological attributes shared across species but exhibited notable differences compared with rat MSNs. We then tested whether MSN electrophysiological properties varied with partner preference strength and found that excitatory synaptic strength (as indicated via mEPSC amplitude) and neuron excitability (as assessed with the slope of the evoked action potential firing rate to depolarizing current injection) correlate with partner preference strength. Additionally, we found that mEPSC amplitude and neuron excitability generally decreased with increasing preference scores. Overall, these data provide, for the first time, detailed methods for whole cell patch-clamp recording from vole acute brain slices and an extensive documentation of vole MSN electrophysiological

characteristics and probe the relationship between MSN electrophysiology and vole partner preference behavior.

## MATERIALS AND METHODS

### Animals

All animal procedures were approved by the North Carolina State University Institutional Animal Care and Use Committee and the resident veterinarian. Prairie voles (*M. ochrogaster*) ($n = 8$) were obtained from a colony housed in the North Carolina State University Biological Resources Facility. Rooms were temperature, humidity, and light controlled (22°C, 30% humidity, 12:12-h light-dark cycle. 6 AM–6 PM lights on). Food (High Fiber Rabbit Diet, 5326, LabDiet; Regular Standard Rodent Chow, 5001, LabDiet; timothy hay, 5LRT, PicoLab, PMI) and water were provided ad libitum. Male ($n = 4$) postnatal day (P)50 Sprague-Dawley CD IGS rats were purchased from Charles River (Raleigh, NC) and housed in same-sex pairs. Age at experimental use ranged from P59 to P67. Rooms were temperature, humidity, and light controlled (23°C, 40% humidity, 12:12-h light-dark cycle). Food (2020X Teklad, Madison, WI) and water were available ad libitum. Dietary differences between voles and rats were unavoidable because of the unique husbandry needs of each species.

### Animal Pairing and Partner Preference Test

At 8–9 wk of age, eight sexually naive males were individually partnered with an adult female for 18 h. Females were injected with 0.1 ml of 20 μg/ml estradiol benzoate (Fisher BioReagents) once a day for the 2 days before pairing to induce ovulation and receptivity toward males. At the end of the 18-h partnering phase, the strength of the male's mate preference was assessed via a partner preference test (PPT) (see Fig. 7A) (Ahern et al. 2009; Slob et al. 1987; Williams et al. 1992). During the PPT, the partner female and an age-matched stranger female never before encountered by the male were tethered at opposite ends of a 0.6 × 0.15 × 0.3-m box. The male was placed in the middle of the cage, and his movements were recorded for 3 h. The time spent by the male in physical contact with his partner female, in physical contact with the stranger female, and alone was analyzed with TopScan (version 3.00), as previously described (Ahern et al. 2009). Partner preference scores were calculated by subtracting the time spent with the stranger from the time spent with the partner, following a published protocol (Slob et al. 1987). Testing was initiated between 8:00 and 8:30 AM. Between testing sessions, the corncob bedding was removed and the arena cleaned with 70% isopropyl alcohol. At the end of the test, each male was returned to his cage with his partner female. Rats did not undergo any behavioral experiments before death because they do not form pair bonds.

### Electrophysiology

*Acute brain slice preparation.* Methods for preparing NAc brain slices for electrophysiological recordings were adapted from previous protocols (Dorris et al. 2014). Animals were deeply anesthetized with isoflurane gas and killed by decapitation. The brain was dissected rapidly into ice-cold, oxygenated (95% $O_2$,-5% $CO_2$) sucrose artificial cerebrospinal fluid (ACSF) containing (in mM) 75 sucrose, 1.25 $NaH_2PO_4$, 3 $MgCl_2$, 0.5 $CaCl_2$, 2.4 Na pyruvate, and 1.3 ascorbic acid from Sigma-Aldrich (St. Louis, MO) and 75 NaCl, 25 $NaHCO_3$, 15 dextrose, 2 KCl from Fisher (Pittsburgh, PA) (osmolarity 295–305 mosM, pH 7.2–7.4). Serial 300-μm coronal brain slices containing the NAc were prepared with a vibratome and incubated in regular ACSF containing (in mM) 126 NaCl, 26 $NaHCO_3$, 10 dextrose, 3 KCl, 1.25 $NaH_2PO_4$, 1 $MgCl_2$, 2 $CaCl_2$ (295–305 mosM, pH 7.2–7.4) for 30 min at 35°C and at least 30 min at room temperature (21–23°C). Slices were stored submerged in room-temperature, oxygenated (95% $O_2$,-5% $CO_2$) ACSF for up to 5 h after sectioning in a large-volume
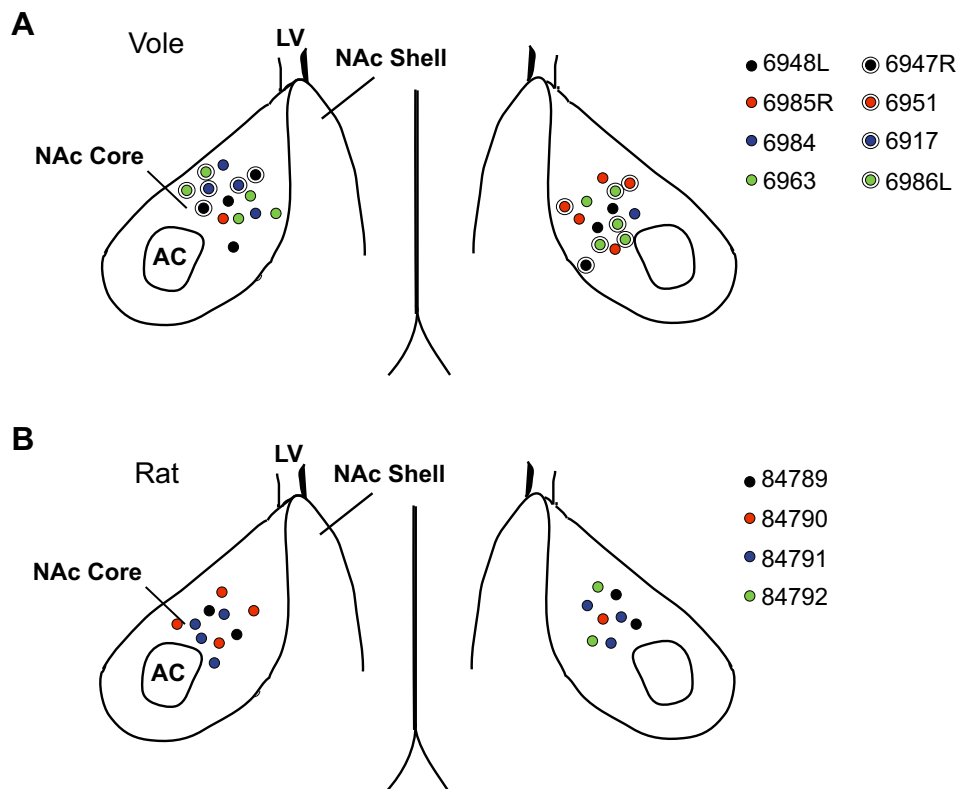
Fig. 1. Nucleus accumbens core (NAc) medium spiny neuron (MSN) map. *A*: location of whole cell patch-clamped MSNs in vole NAc. Four MSNs were recorded from *vole 6948L*, 3 MSNs from *vole 6985R*, 3 MSNs from *vole 6984*, 4 MSNs from *vole 6963*, 3 MSNs from *vole 6947R*, 2 MSNs from *vole 6951*, 2 MSNs from *vole 6917*, and 6 MSNS from *vole 6986L*. *B*: location of whole cell patch-clamped MSNs in rat NAc. Four MSNs were recorded from *rat 84789*, 5 MSNs *rat 84790*, 7 MSNs from *rat 84791*, and 2 MSNs from *rat 84792*. AC, anterior commissure; LV, lateral ventricle.

bath holder. For voles, acute brain slice preparation occurred ~1 h after the PPT.

*Electrophysiological recording.* After resting for ≥1 h after sectioning, slices were placed in a Zeiss Axioscope equipped with IR-DIC optics, a Dage IR-1000 video camera, and ×10 and ×40 lenses with optical zoom. Slices were superfused with oxygenated (95% $O_2$-5% $CO_2$) ACSF heated to 26 ± 1°C. Whole cell patch-clamp recordings were made from MSNs in the NAc (Fig. 1). The NAc was identified with the lateral ventricle and anterior commissure as landmarks. Recordings were made with glass electrodes (4–8 MΩ) containing (in mM) 115 K-D-gluconate, 8 NaCl, 2 EGTA, 2 MgCl$_2$, 2

MgATP, 0.3 NaGTP, and 10 phosphocreatine from Sigma-Aldrich and 10 HEPES from Fisher (285 mosM, pH 7.2–7.4). Signals were amplified, filtered (2 kHz), and digitized (10 kHz) with a MultiClamp 700B amplifier attached to a Digidata 1550 system and a personal computer using pCLAMP 10 software. Membrane potentials were corrected for a calculated liquid junction potential of −13.5 mV, following previous studies (Cao et al. 2016; Dorris et al. 2015; Willett et al. 2016). The following metrics are reported with adjustment for liquid junction potential: resting membrane potential and action potential threshold. Recordings were made initially in current clamp to assess neuronal electrophysiological properties. MSNs were identified

Table 1. *Electrophysiological properties of nucleus accumbens core medium spiny neurons in adult male prairie voles and rats*

| Property | Prairie Vole (P59 ± 3) | Rat (P64 ± 3) | Statistics ($t/U$, $P$) |
|---|---|---|---|
| **Resting potential, mV** | **−86.82 ± 4.69 (28)** | **−89.93 ± 2.57 (18)** | **141.0, 0.01** |
| Delay to first AP, s | 0.42 ± 0.11 (23) | 0.44 ± 0.07 (15) | 172.0, 0.99 |
| **Rheobase, nA** | **0.13 ± 0.06 (28)** | **0.17 ± 0.07 (18)** | **2.15, 0.04** |
| AP threshold, mV | −49.77 ± 7.62 (28) | −50.64 ± 7.51 (18) | 0.38, 0.70 |
| AP amplitude, mV | 60.64 ± 14.09 (28) | 58.09 ± 13.76 (18) | 0.61, 0.55 |
| AP width at half-peak, ms | 2.15 ± 0.82 (28) | 2.15 ± 0.33 (18) | 0.03, 0.98 |
| AHP peak, mV | −8.14 ± 2.43 (28) | −7.91 ± 2.42 (18) | 210.0, 0.35 |
| AHP time to peak, ms | 29.58 ± 12.98 (28) | 30.80 ± 9.26 (18) | 0.34, 0.73 |
| **FI slope, Hz/nA** | **188.06 ± 60.30 (28)** | **153.40 ± 46.75 (18)** | **2.07, 0.04** |
| Linear range input resistance, MΩ | 170.96 ± 75.35 (28) | 143.55 ± 49.17 (18) | 196.0, 0.21 |
| Rectified range input resistance, MΩ | 130.18 ± 46.87 (28) | 123.57 ± 44.69 (18) | 226.0, 0.57 |
| *% Inward rectification* | **78.36 ± 10.60 (28)** | **86.34 ± 10.98 (18)** | **2.46, 0.02** |
| Sag index | 0.008 ± 0.010 (23) | 0.007 ± 0.005 (10) | 103.0, 0.66 |
| Time constant of membrane, ms | 13.55 ± 11.13 (28) | 10.56 ± 4.42 (18) | 235.0, 0.71 |
| Capacitance, pF | 70.72 ± 28.86 (27)* | 77.81 ± 34.25 (18) | 215.0, 0.53 |
| mEPSC frequency, Hz | 3.74 ± 2.76 (23) | 3.30 ± 2.09 (8) | 0.41, 0.69 |
| mEPSC amplitude, pA | 15.41 ± 3.95 (23) | 15.49 ± 3.39 (8) | 0.05, 096 |
| mEPSC decay, ms | 2.98 ± 0.76 (23) | 2.79 ± 0.94 (8) | 0.55, 0.59 |

Values are means ± SD. Numbers in parentheses indicate sample size. Bold font indicates significance. The sag index is unitless. None of these neurons fired spontaneous action potentials. P, postnatal day; AP, action potential; AHP, afterhyperpolarization; FI, frequency of evoked spikes to injected depolarization current; mEPSC, miniature excitatory postsynaptic current. *The vole MSN capacitance data set excluded an outlier that was >15 SD from the mean. Values including the outlier are 87.40 ± 92.67 pF. Statistics are *t*-tests or Mann-Whitney *U*-tests.

by their medium-sized somas, the lack of spontaneous action potential generation, and the presence of at least one of the following characteristics: a slow-ramping subthreshold depolarization in response to low-magnitude positive current injections, a resting potential equaling or more hyperpolarized than −65 mV, and/or inward rectification (Belleau and Warren 2000; Cao et al. 2016; O'Donnell and Grace 1993).

In a subset of recordings, oxygenated ACSF containing the GABA$_A$ receptor antagonist picrotoxin (PTX, 150 $\mu$M; Fisher) and the voltage-gated sodium channel blocker tetrodotoxin (TTX, 1 $\mu$M; Abcam Biochemicals) was applied to the bath to abolish action potentials and inhibitory postsynaptic current events. Once depolarizing current injection no longer elicited an action potential, MSNs were voltage-clamped at −70 mV and mEPSCs were recorded for at least 5 min. These settings make AMPA receptors the likely primary contributor to mEPSC properties. Input and series resistance were monitored for changes, and cells were discarded if resistance changed >25%. mEPSCs were assessed so that any detected difference in synapse property could be linked to pre- and postsynaptic mechanisms. For example, pair bonding could potentially induce differences in either or both AMPA receptor properties and/or excitatory synapse number.

*Data analysis.* Basic electrophysiological properties and action potential characteristics were analyzed with pCLAMP 10. After break-in, the resting membrane potential was first allowed to stabilize for ~1–2 min, following Mu et al. (2010). Three series of 600-ms depolarizing and hyperpolarizing current injections were applied to elicit basic neurophysiological properties. All assessed properties followed the definitions of Willett et al. (2016) and Dorris et al. (2015), which were based upon previous work by Perkel and colleagues (Farries et al. 2005; Farries and Perkel 2000, 2002; Meitzen et al. 2009). Briefly, for each neuron measurements were made of at least three action potentials generated from minimal current injections. These measurements were then averaged to generate the reported action potential measurement for that neuron. Action potential threshold was defined as the first point of sustained positive acceleration of voltage ($\delta^2 V/\delta t^2$) that was also more than three times the SD of membrane noise before the detected threshold (Baufreton et al. 2005). Action potential amplitude was calculated as the difference between threshold and the maximum millivolt value reached at action potential peak. The short afterhyperpolarization peak amplitude was calculated as the difference between the threshold value after the action potential peak and the lowest point after the action potential peak. The slope of the linear range of the evoked firing rate to positive current curve (FI slope) was calculated from the first current stimulus that evoked an action potential to the first current stimulus that generated an evoked firing rate that persisted for at least two consecutive current stimuli. Input resistance in the linear, nonrectified range was calculated from the steady-state membrane potential in response to −0.02-nA hyperpolarizing pulses. Measures of input resistance in the rectified range (rectified range input resistance and percent inward rectification) were calculated from the steady-state membrane potential in response to the most hyperpolarizing current pulse injected into the neuron, following Belleau and Warren (2000). In the present study, this current pulse was −0.14 nA. Percent inward rectification was defined as the rectified range input resistance divided by the linear range input
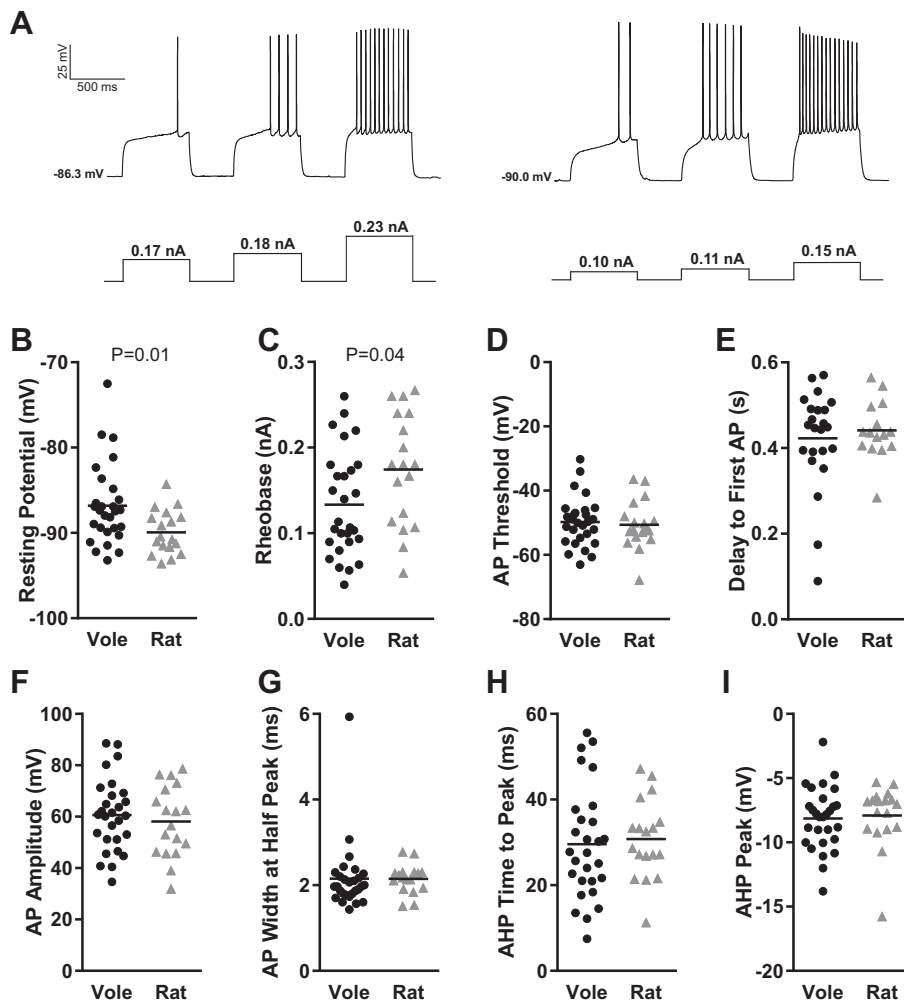


Fig. 2. Vole and rat MSN action potential properties. *A*: voltage response of 2 different vole MSNs (*left* and *right*) to a series of depolarizing current injections. *B*: membrane resting potential. *C*: rheobase. *D*: action potential (AP) threshold. *E*: delay to first action potential. *F*: action potential amplitude. *G*: action potential width measured at half-peak action potential amplitude. *H*: action potential afterhyperpolarization (AHP) time to peak. *I*: action potential afterhyperpolarization peak amplitude. Horizontal line in *B–I* indicates mean. Complete action potential properties are documented in Table 1.
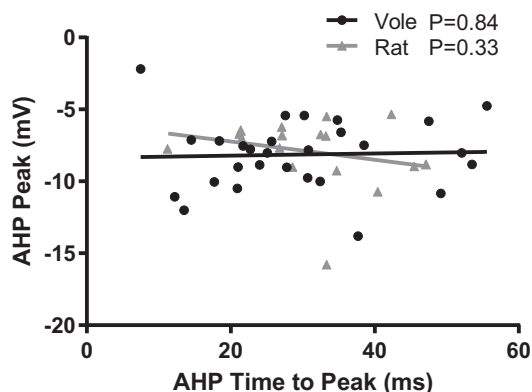
Fig. 3. Vole and rat MSN action potential afterhyperpolarization properties do not correlate with one another. Line indicates best fit. Complete statistical information is located in RESULTS.

resistance multiplied by 100. A neuron with no rectification will have a percent inward rectification of 100%. A neuron exhibiting rectification will have a small percent inward rectification score. The membrane time constant was calculated by fitting a single exponential curve to the membrane potential change in response to $-0.02$-nA hyperpolarizing pulses. Membrane capacitance was calculated with the following equation: capacitance = membrane time constant/input resistance. Sag index was used to assess the presence of hyperpolarization-induced "sag" (i.e., $I_H$ current), which is uncommon in rat and mice MSNs but has been detected in chicken (Farries et al. 2005). Sag index is the difference between the minimum voltage measured during the largest hyperpolarizing current pulse and the steady-state voltage deflection of that pulse divided by the steady-state voltage deflection. Thus a cell with no sag would have a sag index of $\leq 0$, whereas a cell whose maximum voltage deflection is twice that of the steady-state deflection would have a sag index of 1. Cells with considerable sag

typically have an index of $\geq 0.1$. Sag index was only calculated for cells for which the minimum voltage was lower than the steady-state voltage deflection of the largest hyperpolarizing current pulse. mEPSC frequency, amplitude, and decay were analyzed with Mini Analysis (Synaptosoft, http://www.synaptosoft.com/MiniAnalysis/), following Cao et al. (2016). Recordings were filtered (1 kHz), and mEPSC threshold was set at a minimum value of 5 pA. Accurate event detection was validated by visual inspection.

### Statistics

Experiments were analyzed with two-tailed *t*-tests, Mann-Whitney *U* tests, two-way repeated-measures ANOVA, and linear regressions. Pearson or Spearman correlations were employed for parametric and nonparametric data sets, respectively (Prism version 6.0; GraphPad Software, La Jolla, CA). Distributions were analyzed for normality with the D'Agostino and Pearson omnibus normality test. *P* values $<$ 0.05 were considered a priori as significant and *P* values $<$ 0.10 as a trend. Data are presented as means $\pm$ SD.

### RESULTS

To meet our primary goal of understanding the properties of prairie vole MSNs, we recorded 28 MSNs from the NAc of eight adult males. Aggregate electrophysiological properties of the recorded MSNs are provided in Table 1.

### Medium Spiny Neuron Action Potential Properties

We first analyzed resting membrane potential and action potential properties (Fig. 2*A*). The canonical hyperpolarized resting membrane potential found in MSNs in acute brain slice preparation (Calabresi et al. 1987; Wilson and Groves 1981) was found to be highly conserved in vole MSNs, in the sense
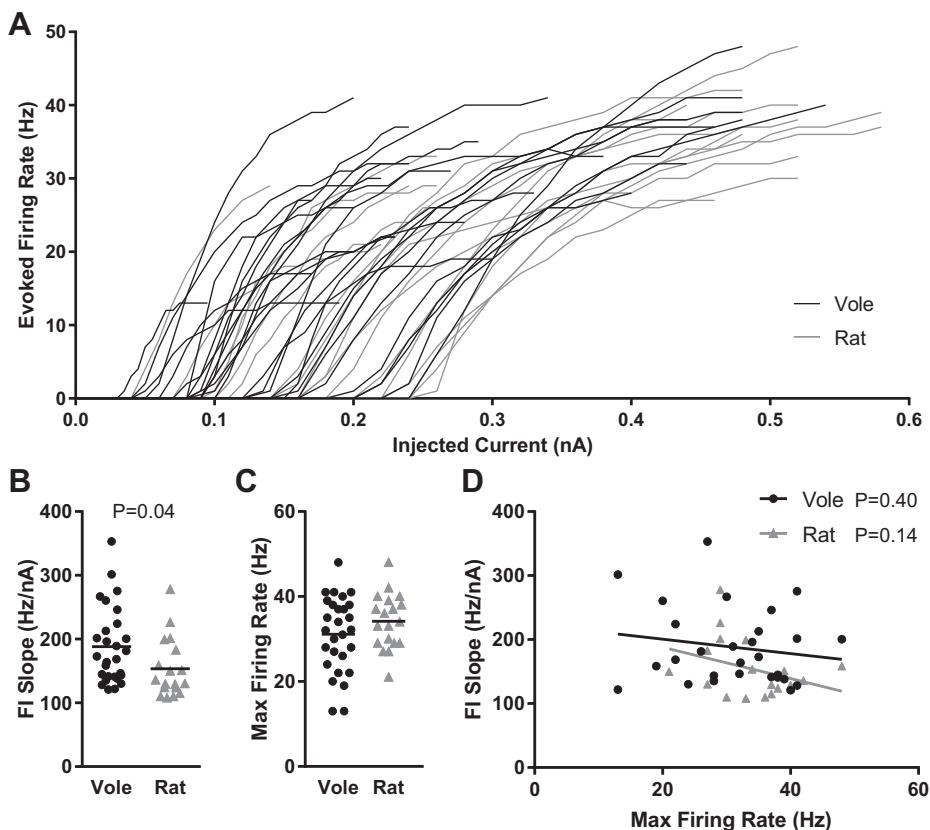


Fig. 4. Vole and rat MSN excitability. *A*: action potential firing rates evoked by depolarizing current injection. *B*: slopes of the evoked firing rate-to-positive current curve (FI slope) for individual vole and rat MSNs. *C*: maximum action potential firing rate evoked by depolarizing current injection. *D*: FI slope and maximum action potential firing rate do not correlate with one another. Horizontal line in *B* and *C* indicates mean; the lines in *D* indicate best fit. Complete MSN excitability properties and statistics are documented in Table 1.

that no MSN exhibited a resting membrane potential of greater than −70 mV after liquid junction potential correction (Fig. 2B). Vole MSNs did show a wider range in resting membrane potential compared with rat MSNs. This difference in range led to the detection of a significant difference in resting membrane potential between voles and rats ($P = 0.01$, Mann-Whitney $U$-test; complete statistical information for this and all other comparisons is in Table 1). A significant difference was also detected in rheobase (Fig. 2C; $P = 0.04$, $t$-test), but without the accompanied difference in range. Action potential threshold was relatively similar between species (Fig. 2D). MSN delay to first action potential was likewise highly conserved across species (Fig. 2E). This property is another canonical feature of MSNs and reflects the magnitude of the slowly inactivating A current, also called the voltage-gated transient A-type K current, responsible for the slow ramping subthreshold depolarization (Nisenbaum et al. 1994). Interestingly, most but not all vole and rat MSNs showed this delay. Among the MSNs that did show a delay, this ranged over 200 ms, demonstrating substantial potential variation in A-current properties across species. Other action potential properties did not differ by species, including action potential amplitude (Fig. 2F) and width (Fig. 2G). Regarding action potential afterhyperpolarization, this varied widely among both vole and rat MSNs. Vole and rat MSNs demonstrated an ~40-ms range in time to peak

afterhyperpolarization (Fig. 2H) and both large and small afterhyperpolarization peak size (Fig. 2I). Afterhyperpolarization time to peak amplitude and peak amplitude did not correlate in either rat or vole MSNs (Fig. 3), suggesting that these properties are controlled by separate mechanisms. This is consistent with the diversity of ion channels regulating specific components of rat neostriatum MSN afterhyperpolarization (Galarraga et al. 1989; Pineda et al. 1992). Overall, these findings indicate that vole MSNs generally exhibit the canonical MSN action potential properties. However, the magnitude of these properties varies substantially between individual MSNs and in some cases differs in degree from those assessed in rat MSNs.

### Medium Spiny Neuron Excitability

We then analyzed overall MSN excitability by plotting the frequency of action potentials evoked by depolarizing current injection curve (FI curve) for individual vole and rat MSNs (Fig. 4A). Note that Fig. 4A depicts FI curves up to MSN maximum firing rate. After that point, MSNs either decreased firing rates or stopped generating action potentials in response to depolarizing current injections. We quantified individual MSN excitability by calculating the slope of the evoked firing rate to positive current curve (FI slope; Fig. 4B), and maximum
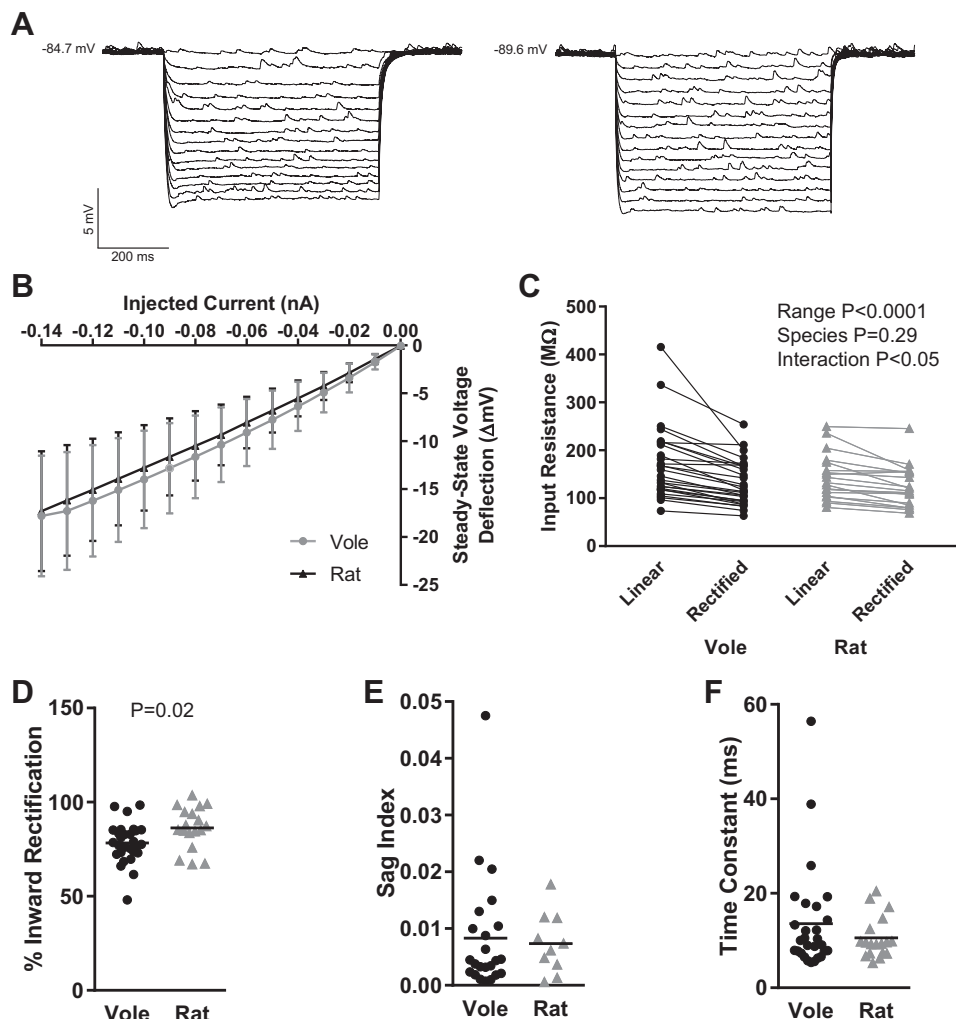


Fig. 5. Vole and rat MSN passive electrophysiological properties. A: voltage response of 2 individual vole MSNs (*left* and *right*) to a series of hyperpolarizing current injections. Note that MSN on *left* exhibits increased inward rectification (~66% inward rectification) compared with MSN on *right* (~85% inward rectification). B: vole and rat MSNs, in general, exhibited inward rectification in response to hyperpolarizing current injections but showed substantial individual variability in voltage deflection as indicated by the standard deviations. C: vole and rat MSNs generally exhibit input resistance that varies strongly with membrane potential. However, extensive variation per individual MSN was present, including a subpopulation of MSNs that did not exhibit varying input resistance at all, leading to an interaction effect between input resistance, range, and species. D: % inward rectification. E: sag index. F: time constant of the membrane. Horizontal line in D–F indicates mean. Complete MSN passive properties and statistics are documented in Table 1.

firing rate (Fig. 4C). This quantification revealed a significant difference between rat and vole MSNs ($P = 0.04$, $t$-test), with vole MSNs exhibiting steeper FI slopes, indicating greater excitability in vole MSNs. In both vole and rat MSNs, FI slope and maximum firing rate properties did not correlate with each other, suggesting that they are mediated by separate subcellular mechanisms (Fig. 4D). Overall, these data indicate that excitability differs markedly between individual MSNs in both voles and rats and that vole MSNs are on average more excitable than rat MSNs.

### Medium Spiny Neuron Passive Properties: Input Resistance and Inward Rectification

In response to hyperpolarizing current pulses, MSNs typically exhibit input resistance that varies strongly with membrane potential and marked time-independent inward rectification that is especially noticeable at highly negative membrane potentials. We assessed these properties in vole and rat MSNs by injecting a series of increasingly hyperpolarizing current pulses (Fig. 5A). Considered as a population (Fig. 5B), vole MSNs generally exhibited both varying input resistance and inward rectification, as found in MSNs from rats. However, small subpopulations of vole MSNs did not exhibit varying input resistance (Fig. 5C; $n = 4$ MSN with $\leq$10-mV difference between linear range input resistance and rectified range input resistance), leading to an interaction effect when the data were analyzed with a repeated-measures two-way ANOVA with input resistance range and species as factors [interaction: $F_{(1,45)} = 4.2$, $P < 0.05$; input resistance range: $F_{(1,45)} = 35.6$, $P < 0.0001$; species: $F_{(1,45)} = 1.1$, $P > 0.05$; subjects (matching): $F_{(45,45)} = 9.9$, $P < 0.0001$]. To further assess the robustness of this finding, we further analyzed inward rectification by calculating percent inward rectification, which was significantly lower in vole MSNs compared with rat MSNs ($P = 0.02$, $t$-test; Fig. 5D; percent inward rectification = rectified range input resistance/linear range input resistance $\times$ 100). In the example traces in Fig. 5A, the trace on the left has a percent inward rectification of 66%, while the trace on the right that shows less rectification has a percent inward rectification of 85%. A small number of vole MSNs also exhibited small but noticeable time-dependent inward rectification, which was not present in rat MSN recordings but has been documented in subpopulations of chick MSNs (Farries et al. 2005). In this case, the membrane potential sharply depolarizes to a new steady-state level soon after initial hyperpolarization, so that a "sag" is present in the MSN's voltage response to an inhibitory
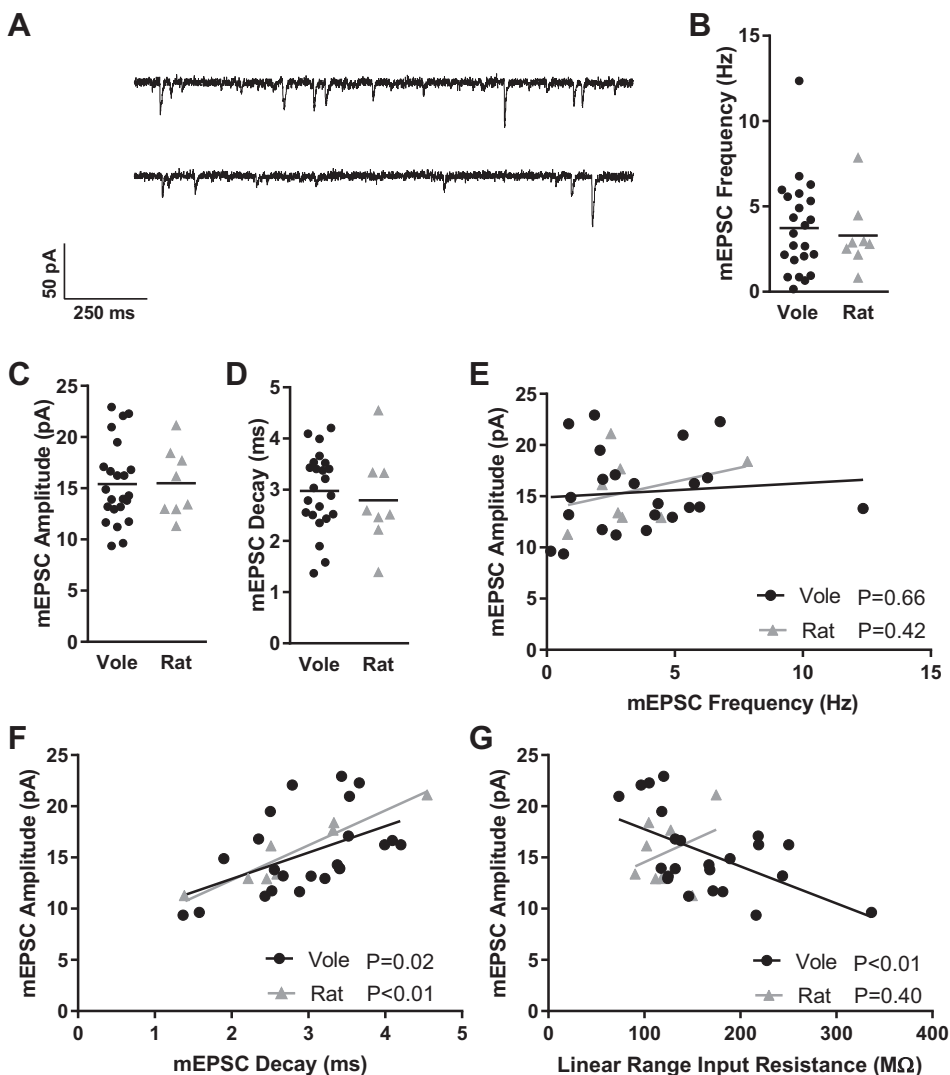


Fig. 6. Vole and rat MSN mEPSC properties. A: representative examples of mEPSCs recorded from 2 different vole MSNs. MSNs were voltage clamped at −70 mV and recorded in the presence of TTX and PTX to block voltage-gated sodium channels and GABAergic synaptic activity, respectively. B: mEPSC frequency. C: mEPSC amplitude. D: mEPSC decay. E: for both voles and rats, mEPSC amplitude and frequency do not correlate with one another. F: mEPSC amplitude and mEPSC decay correlate with one another in both species, indicating that bigger mEPSCs typically require more time to decay to baseline voltage. G: mEPSC amplitude and linear range input resistance inversely correlate in voles, surprisingly indicating that MSNs exhibiting larger-amplitude mEPSCs have lower input resistances. Horizontal line in B–D indicates mean. Lines in E–G indicate best fit. Complete MSN mEPSC properties and statistics are documented in Table 1.

current pulse. To measure this phenomenon, we quantified sag index, a unitless metric that increases with the amount of sag (Fig. 5E). Three MSNs recorded from different voles showed sag index of ≥0.02. To complete our characterization of vole MSN passive properties, we measured the time constant of the membrane, which did not differ between vole and rat MSNs (Fig. 5F). Similar to rat MSNs, vole MSNs exhibited relatively shorter membrane time constants, although there were a handful of outlier MSNs with longer time constants. These outlier MSNs were recorded from different voles and were not the same MSNs that showed a sag index ≥0.02. Overall, vole MSNs showed passive properties similar to those found in rats, with increased variability in the degree of inward rectification within individual MSNs.

*Medium Spiny Neuron mEPSC Properties*

Vole and rat MSNs exhibited similar mEPSC characteristics (Fig. 6A). mEPSC frequencies, for instance, varied from almost 0 Hz to over 10 Hz in both vole and rat MSNs (Fig. 6B). mEPSC amplitude (Fig. 6C) and decay (Fig. 6D) were also variable within a species but did not differ between species. As expected, mEPSC amplitude and frequency did not correlate for either species (Fig. 6E; $F = 0.198$, $R^2 = 0.01$, $P > 0.66$, Pearson correlation), while mEPSC amplitude and decay did for both (Fig. 6F; $F = 6.895$, $R^2 = 0.25$, $P < 0.02$, Pearson correlation), meaning that bigger mEPSC events typically required more time to decay back to baseline than smaller mEPSC events. Unexpectedly, in vole MSNs but not rat MSNs there was an inverse relationship between mEPSC amplitude and both linear range input resistance (Fig. 6G; $F = 9.628$, $R^2 = 0.31$, $P < 0.01$, Pearson correlation) and rectified range input resistance (data not shown; $F = 16.41$, $R^2 = 0.44$, $P < 0.01$, Pearson correlation), in that vole MSNs with higher input

resistances tended to have smaller mEPSC amplitudes. It is possible that this relationship may also be present in rat MSNs, but our experiment does not possess sufficient power to detect this relationship. In vole MSNs, this positive correlation suggests that some form of homeostatic or another type of scaling plasticity may be present.

*Partner Preference Behavior*

Four male voles spent more time with their partner females (Fig. 7B) and thus showed a strong positive preference for their partnered female (Fig. 7C). The other four male voles spent significantly more time alone (Fig. 7B), and thus showed no preference (a score near 0; Fig. 7C), or spent significantly more time with the stranger female (Fig. 7B), and thus showed a preference for the stranger female (a negative preference score; Fig. 7C).

*Partner Preference Behavior and MSN Electrophysiological Properties*

mEPSC amplitude decreased with preference score, both when calculated as an average value for each animal (i.e., each vole is considered an experimental unit; the values for all the neurons recorded from each animal were averaged to yield a single mean per animal) (Fig. 8A, *left*; $F = 5.38$, $R^2 = 0.47$, $P = 0.06$, Pearson correlation, trend) and when calculated with values for each neuron (i.e., each neuron is considered an experimental unit) (Fig. 8A, *right*; $F = 4.75$, $R^2 = 0.18$, $P = 0.04$, Pearson correlation, significant). This indicates that the excitatory synaptic strength, most probably postsynaptic MSN expression and/or availability of AMPA receptors, decreases with stronger preference for the partner female. Unexpectedly, FI slope, a measure of neuron excitability, also decreased with
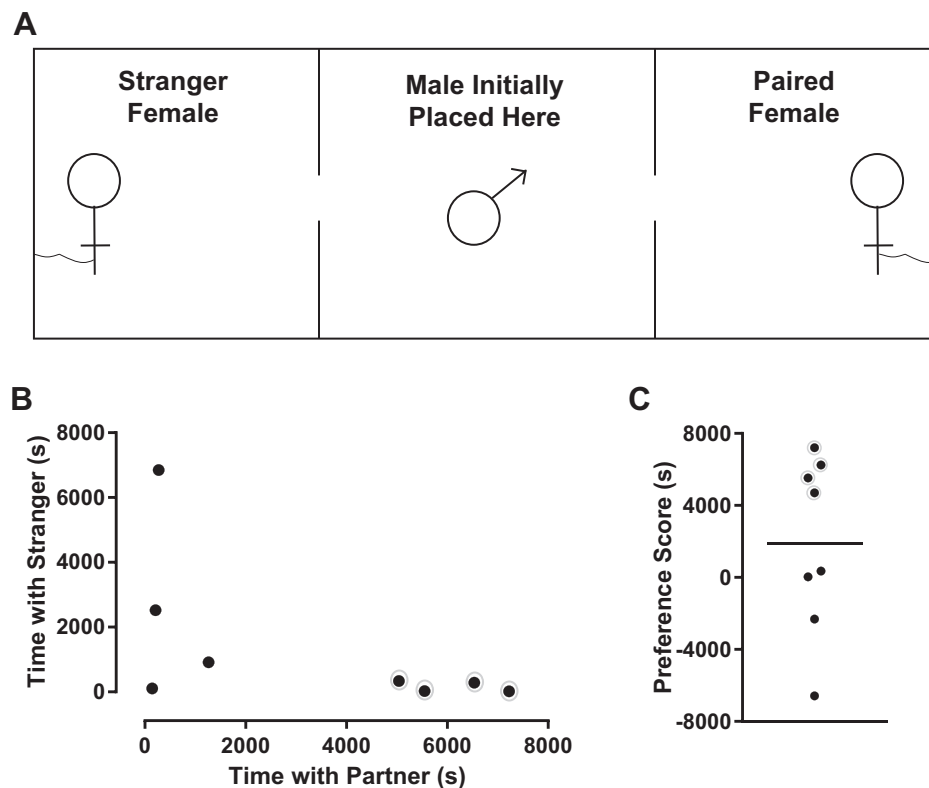
Fig. 7. Vole partner preference test apparatus and behavior. *A*: top-down view of the partner preference test apparatus. A male vole was placed in the middle of a $0.6 \times 0.15 \times 0.3$-m box, and his movements were recorded for 3 h (10,800 s). His partnered female and a stranger female never before encountered by the male were tethered at opposite ends of the box. The time spent by the male in physical contact with his partner female, in physical contact with the stranger female, and alone was analyzed. *B*: 4 of the 8 male voles spent the vast majority of time in physical contact with the partnered female, indicated by a gray circle around the respective data points. *C*: individual vole preference scores. Positive preference score indicates that male vole spent more time with partnered female than stranger female (these voles again indicated with gray circles). Negative score indicates that male spent more time with stranger female. Horizontal line in *C* indicates mean.

Fig. 8. Relationship of vole MSN mEPSC amplitude and FI slope to partner preference behavior. *A*: mEPSC amplitude magnitudes decrease with larger preference scores. *Left*: mEPSC amplitudes calculated as an average value ± SE for each vole. *Right*: mEPSC amplitudes calculated using values for individual neurons. *B*: FI slope magnitudes decrease with larger preference scores. *Left*: FI slopes calculated as an average ± SE for each vole. *Right*: FI slopes calculated using values for individual neurons. Note that there is no best-fit line because of the Spearman's correlation employed. *C*: mEPSC amplitude and FI slope magnitudes decrease with each other. *Left*: mEPSC amplitudes and FI slopes calculated as average values ± SE for individual voles. *Right*: mEPSC amplitudes and FI slopes calculated as average value for individual MSNs. Note that there is no best-fit line because of the Spearman's correlation employed. Gray circles indicate vole with strong preference scores, as in Fig. 7. Best-fit lines are depicted for Pearson's correlations only. Complete statistical information is located in Table 2.
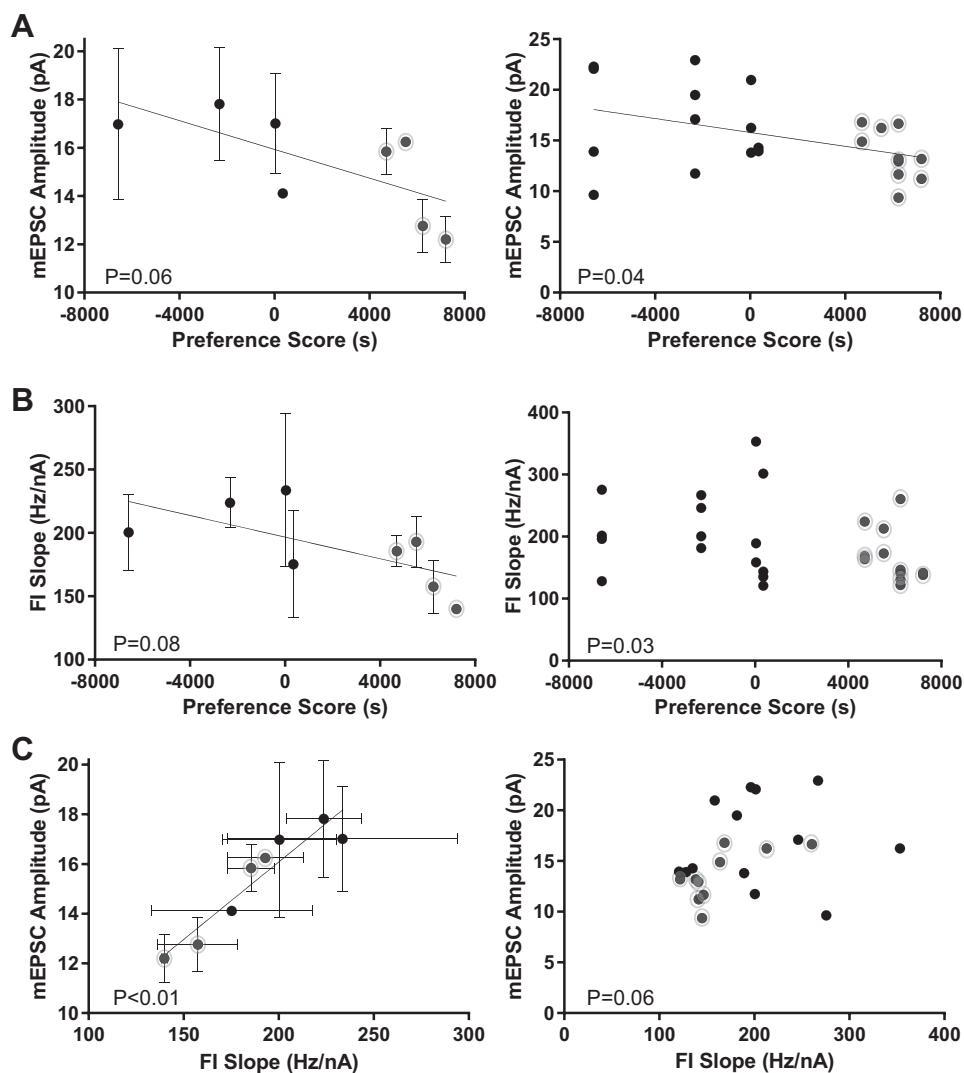
preference score, indicating decreased intrinsic excitability with stronger preference for the partner female (Fig. 8*B*, *left*; calculated per animal; $F = 4.502$, $R^2 = 0.43$, $P = 0.08$, Pearson correlation, trend) (Fig. 8*B*, *right*; calculated per neuron; $R = -0.42$, $P = 0.03$, no regression line shown because of Spearman correlation, significant). If both FI slope and mEPSC amplitude values correlate with preference score, then this predicts that FI slope and mEPSC amplitude should likewise correlate with each other. This relationship was confirmed, with increased FI slope values associating with increased mEPSC amplitude values, either when calculated per animal (Fig. 8*C*, *left*; $F = 44.62$, $R^2 = 0.88$, $P < 0.01$, Pearson correlation, significant) or per neuron (Fig. 8*C*, *right*; $R = 0.40$, $P = 0.06$; no regression line shown because of Spearman correlation, trend). Overall, these findings indicate that in male vole MSNs decreased neuronal excitability is correlated with increased preference for the partnered female.

## DISCUSSION

Vole MSNs largely exhibit the defining characteristics of spiny striatal neurons common to vertebrate taxa, indicating that MSN electrophysiology is largely evolutionarily conserved. In mammals, songbirds and non-songbirds, and rep-

tiles, MSNs exhibit a medium-sized soma and the following properties: slow-ramping subthreshold depolarization in response to low-magnitude positive current injections, a hyperpolarized resting potential, decreasing input resistance with greater hyperpolarizing inputs (inward rectification), and noticeable action potential afterhyperpolarization (Cepeda et al. 1994). Some prairie vole MSNs, however, exhibited varying degrees of or even complete absence of select electrophysiological properties.

Vole NAc MSNs exhibited stable resting membrane potentials over a greater range than rat NAc MSNs. While the majority of vole MSNs rested around −90 mV, a subpopulation of MSNs rested at a more depolarized potential around −80 mV not seen in the rat data set. Interestingly, vole NAc MSNs required less positive current stimulus to elicit an action potential than rat NAc MSNs on average, but vole and rat NAc MSN action potential thresholds did not differ. Furthermore, vole NAc MSNs demonstrated an increased rate of action potential production relative to rat NAc MSNs, but the maximum firing rate acquired by MSNs did not differ between rats and voles. Concomitantly, vole NAc MSNs exhibit a lower percentage of inward rectification than rat MSNs. Taken together, these findings suggest that subtle differences in cellular

Table 2. *Relationship between prairie vole MSN electrophysiological properties and partner preference behavior*

| Property | Correlates with Preference Score? | |
| --- | --- | --- |
| | Neuron analysis | Animal analysis |
| Resting potential, mV | $R = 0.23†, P > 0.23$ | $R = -0.02*, P > 0.97$ |
| Delay to first AP, s | $R = 0.01†, P > 0.95$ | $R = -0.01*, P > 0.99$ |
| Rheobase, nA | $R = 0.08*, P > 0.70$ | $R = 0.11*, P > 0.79$ |
| AP threshold, mV | $R = 0.31*, P > 0.11$ | $R = 0.28*, P > 0.50$ |
| AP amplitude, mV | $R = -0.28*, P > 0.15$ | $R = -0.32*, P > 0.43$ |
| AP width at half-peak, ms | $R = 0.18*, P > 0.36$ | $R = 0.64†, P > 0.10$ |
| AHP peak, mV | $R = -0.18*, P > 0.35$ | $R = -0.49*, P > 0.22$ |
| AHP time to peak, ms | $R = 0.08*, P > 0.68$ | $R = -0.05*, P > 0.90$ |
| **FI slope, Hz/nA** | **$R = -0.42†, P < 0.03$** | **$R = -0.65*, P < 0.08$** |
| Linear range input resistance, MΩ | $R = 0.18†, P > 0.35$ | $R = -0.02*, P > 0.95$ |
| Rectified range input resistance, MΩ | $R = 0.03*, P > 0.89$ | $R = -0.07*, P > 0.86$ |
| % Inward rectification | $R = -0.01*, P > 0.94$ | $R = -0.23*, P > 0.58$ |
| Sag index | $R = 0.37†, P > 0.09$ | $R = 0.62†, P > 0.12$ |
| Time constant of membrane, ms | $R = -0.26†, P > 0.18$ | $R = -0.52†, P > 0.20$ |
| Capacitance, pF | $R = -0.13†, P > 0.53$ | $R = -0.43*, P > 0.28$ |
| mEPSC frequency, Hz | $R = -0.01†, P > 0.95$ | $R = 0.07†, P > 0.88$ |
| **mEPSC amplitude, pA** | **$R = -0.43*, P < 0.04$** | **$R = -0.69*, P < 0.06$** |
| mEPSC decay, ms | $R = -0.08*, P > 0.71$ | $R = -0.06*, P > 0.88$ |

Bold font indicates significance or trend. *Pearson or †Spearman correlations were computed as appropriate.

physiology such as ion channel composition and/or soma size or some other property exist between vole and rat NAc MSNs that underlie the select differences observed here.

Some of these species differences are driven by a subset of MSNs in the vole population. Possibly, this subset of MSNs either are not MSNs or represent a different subtype of MSNs. The preponderance of evidence, however, indicates that these two explanations are unlikely. The canonical electrophysiological properties of the MSN are a slow-ramping subthreshold depolarization in response to low-magnitude positive current injections, a hyperpolarized resting potential, decreasing input resistance with greater hyperpolarizing inputs (inward rectification), and noticeable action potential afterhyperpolarization. When considered as a population, vole MSNs matched this rather established paradigm, although some individual neurons exhibited variability in these characteristics. Importantly, no MSN recorded lacked all of these features, and most MSNs exhibited all of them, demonstrating that all of the recorded neurons are indeed MSNs.

Furthermore, no recorded neuron exhibited the features of rare striatal interneurons found in other rodents. However, our recording paradigm would have biased against detection of these interneurons, and we believe that they are present. Although we characterize all of the recorded MSNs as a single class, MSN subtypes have been detected in other rodents (Gertler et al. 2008; Planert et al. 2013; Staffend et al. 2014), and these subtypes have subtle electrophysiological differences and there is likewise no reason to believe that they are absent from vole striatum. With that limitation acknowledged, we conclude it unlikely that the electrophysiological differences detected here are explained by differential sampling of D1 vs. D2 receptor-expressing MSNs. In rats, D1 vs. D2 dopamine receptor-expressing MSNs showed differences in passive membrane properties including depolarized-range input resis-

tance, the membrane time constant, and rheobase (Planert et al. 2013), similar but not identical to previous findings in mice (Ade et al. 2011; Cepeda et al. 2008; Gertler et al. 2008; Ma et al. 2012). We detected no divergence in the data set of these properties that would clearly delineate between the two MSN subtypes or drive significant differences between voles and rats.

Regarding social behavior, the diversity in behavior displayed by voles is thought to play an advantageous ethological function in the wild (Perkeybile and Bales 2017). Typically, male voles either become a resident defender of a physical territory or wander between territories. Those that become resident defenders either join a female to create a male-female breeding pair or join a communal group comprised of a male-female breeder pair and several alloparents (Getz and Carter 1996). Male voles that wander do not defend a defined territory (Getz et al. 1993; McGuire and Getz 2010). Within the resident strategy, some males will have extrapair copulations, while other males will only mate with their respective paired female (Okhovat et al. 2015; Ophir et al. 2008). This variability in behavior was reflected in the results of our study, in that four of eight males showed a strong preference for their partnered female while four others did not. This spectrum of partner preference provided a useful backdrop in which to test the hypothesis that NAc MSN electrophysiological properties varied with partner preference strength.

NAc MSNs receive substantial excitatory synaptic input from a variety of afferent sources, and this excitatory synaptic input plays a key role in driving MSN action and membrane potential physiology (Gruber and O'Donnell 2009; Wilson 2017; Wilson and Groves 1981). Excitatory synaptic input onto MSNs has also been shown to be a key target of plasticity, with differences detected in both natural and pathological reinforcers (Britt et al. 2012; Wolf 2010) and by sex (Cao et al. 2016; Wissman et al. 2011). Thus the nucleus accumbens' function as a nexus between the limbic, dopaminergic, and motor pathways led to the a priori prediction that excitatory synaptic input onto NAc MSNs would be the most likely properties associated with partner preference, especially since previous studies implicated dopaminergic signaling in the nucleus accumbens shell subregion as necessary for pair bond formation in prairie voles. Consistent with this prediction, mEPSC amplitude and FI slope tended to decrease with increased partner preference. These characteristics are both related to overall neuronal excitability. Regarding mEPSC amplitude, the recording technique employed here targets events related to the expression of AMPA/kainate receptors on the postsynaptic side of glutamatergic synapses, although it remains possible that presynaptic quantal content may have decreased. Lower-amplitude mEPSCs typically indicate that fewer AMPA/kainate receptors are present. FI slope provides a different window onto MSN excitability by directly assessing the input-output relationship of the neuron. A lower FI slope indicates that fewer action potentials are generated per input current, and when this decrease in output is coupled with decreased mEPSC amplitude (aka a decrease in input) this may have large-magnitude effects on the neuron's in vivo physiology. Amadei et al. found that increased entrainment between the mPFC and the NAc biases partner preference behaviors in female voles (Amadei et al. 2017). As discussed above, our study found a negative relationship between partner preference behavior, mEPSC amplitude, and FI slope in male

voles. Taken together, these findings suggest at least two possible hypotheses: there is a sex difference present in voles, or there is homeostatic plasticity at play and the MSN is adapting to the increased excitatory synaptic activation by decreasing cellular excitability. Further analyses of spontaneous or evoked EPSCs could help inform these hypotheses. While in acute brain slice preparations MSNs are usually quiescent, in vivo MSNs show episodic, seconds-long, high-frequency action potential generation associated with specific motivational, motor, and/or sensorimotor events (Kimura 1990; Kimura et al. 1990; Opris et al. 2011). Thus a decrease in the input-output relationship may decrease the neuron's effective firing rate to these stimuli.

Given that dopaminergic signaling in the nucleus accumbens shell and not the NAc is necessary for partner preference formation (Aragona et al. 2006), our favored interpretation is that these electrophysiological changes in excitability do not reflect necessary electrophysiological properties for pair bond formation. The NAc and shell subregions have very clear inputs and outputs (Heimer et al. 1991; Zahm and Heimer 1993), among other differences. The NAc is more closely intertwined with striatal motor pathways and is thought to mediate integrating motivational stimuli into motor actions. The shell, on the other hand, is more closely associated with limbic regions and is thought to compute affect-related signals, as well as processing relevant environmental stimuli (Jean-blanc et al. 2002; Meredith et al. 2008; Zahm and Brog 1992). Thus we speculate that these changes in excitability are related to the premotor actions produced by increased partner preference. Indeed, silencing NAc neurons with procaine decreases spontaneous locomotion and amphetamine-induced locomotion in male rats (Ikemoto and Witkin 2003), and lesions of the NAc and the nucleus accumbens in general change spontaneous locomotor activity (Kelly and Roberts 1983; Parkinson et al. 1999).

An important consideration necessary to put the findings of this experiment in context relates to the differences in social experience between voles and rats. It is possible that these electrophysiological changes are related to a partner preference-related reward stimulus, such as that associated with sexual experience. The nucleus accumbens mediates many naturally rewarding behaviors, including feeding, drinking, maternal behavior, and, most notable for the present study, sexual reward (Bradley et al. 2005; Numan 2007; Pitchers et al. 2010; Vucetic and Reyes 2010; Yoshida et al. 1992; Young and Wang 2004). The rats used in this study were sexually naive. The voles used in this study were also sexually naive before experimental use. Thus any sexual experience gained by the voles over the 18-h partnering period would have been a novel stimulus and possibly reflected in MSN properties. It has been shown that male or female sexual experience increases the density of dendritic spines on NAc but not nucleus accumbens shell MSNs in hamsters and rats (Meisel and Mullins 2006; Pitchers et al. 2010; Staffend et al. 2014), a change normally associated with mEPSC frequency. However, mEPSC frequency did not associate with partner preference in voles, and no difference in mEPSC frequency was detected between voles and rats, despite differences in sexual experience. This is in some ways similar to the findings of a study in rats that found no difference in the membrane expression of AMPA subunits GluA1 and GluA2 in the entire

nucleus accumbens 1 day after sex exposure, although subunit expression changed 1 wk after mating activity (Pitchers et al. 2012). With this acknowledged, there still could be a baseline difference in dendritic spine density that exists independently of the number of excitatory synapses, or there are species differences in spine density or excitatory synaptic properties that would mask the effects of sexual reward. Future studies should address these possibilities.

To conclude, male vole NAc MSN intrinsic electrophysiological properties were largely consistent with those observed in rats and other mammalian species. Notably, vole MSNs were significantly more excitable than rat MSNs as evident by a depolarized resting membrane potential, decreased rheobase, increased FI slope, and decreased percent inward rectification relative to rats. Furthermore, our data provide evidence that select MSN properties in the NAc vary with partner preference strength in males. Specifically, mEPSC amplitude and FI slope tend to decrease with increased partner preference. Future experiments that assess the relationship between the electrophysiological properties of neurons in other brain regions involved in pair bond formation and maintenance, as well as in females, and partner preference behavior would greatly inform the results presented here.

## DISCLOSURES

No conflicts of interest, financial or otherwise, are declared by the authors.

## AUTHOR CONTRIBUTIONS

J.A.W. conceived and designed research; J.A.W. performed experiments; J.A.W., A.G.J., and J.M. analyzed data; J.A.W., A.R.V., H.B.P., L.A.M., and J.M. interpreted results of experiments; J.A.W. and J.M. prepared figures; J.A.W. and J.M. drafted manuscript; J.A.W., A.G.J., A.R.V., H.B.P., L.A.M., and J.M. edited and revised manuscript; J.A.W., A.G.J., A.R.V., H.B.P., L.A.M., and J.M. approved final version of manuscript.

## REFERENCES

**Ade KK, Wan Y, Chen M, Gloss B, Calakos N.** An improved BAC transgenic fluorescent reporter line for sensitive and specific identification of striatonigral medium spiny neurons. *Front Syst Neurosci* 5: 32, 2011. doi:10.3389/fnsys.2011.00032.

**Ahern TH, Modi ME, Burkett JP, Young LJ.** Evaluation of two automated metrics for analyzing partner preference tests. *J Neurosci Methods* 182: 180–188, 2009. doi:10.1016/j.jneumeth.2009.06.010.

**Amadei EA, Johnson ZV, Jun Kwon Y, Shpiner AC, Saravanan V, Mays WD, Ryan SJ, Walum H, Rainnie DG, Young LJ, Liu RC.** Dynamic corticostriatal activity biases social bonding in monogamous female prairie voles. *Nature* 546: 297–301, 2017. doi:10.1038/nature22381.

**Aragona BJ, Liu Y, Curtis JT, Stephan FK, Wang Z.** A critical role for nucleus accumbens dopamine in partner-preference formation in male prairie voles. *J Neurosci* 23: 3483–3490, 2003.

**Aragona BJ, Liu Y, Yu YJ, Curtis JT, Detwiler JM, Insel TR, Wang Z.** Nucleus accumbens dopamine differentially mediates the formation and

maintenance of monogamous pair bonds. *Nat Neurosci* 9: 133–139, 2006. doi:10.1038/nn1613.

**Barrett CE, Keebaugh AC, Ahern TH, Bass CE, Terwilliger EF, Young LJ.** Variation in vasopressin receptor (Avpr1a) expression creates diversity in behaviors related to monogamy in prairie voles. *Horm Behav* 63: 518–526, 2013. doi:10.1016/j.yhbeh.2013.01.005.

**Baufreton J, Atherton JF, Surmeier DJ, Bevan MD.** Enhancement of excitatory synaptic integration by GABAergic inhibition in the subthalamic nucleus. *J Neurosci* 25: 8505–8517, 2005. doi:10.1523/JNEUROSCI.1163-05.2005.

**Belleau ML, Warren RA.** Postnatal development of electrophysiological properties of nucleus accumbens neurons. *J Neurophysiol* 84: 2204–2216, 2000. doi:10.1152/jn.2000.84.5.2204.

**Bosch OJ, Nair HP, Ahern TH, Neumann ID, Young LJ.** The CRF system mediates increased passive stress-coping behavior following the loss of a bonded partner in a monogamous rodent. *Neuropsychopharmacology* 34: 1406–1415, 2009. doi:10.1038/npp.2008.154.

**Bradley KC, Boulware MB, Jiang H, Doerge RW, Meisel RL, Mermelstein PG.** Changes in gene expression within the nucleus accumbens and striatum following sexual experience. *Genes Brain Behav* 4: 31–44, 2005. doi:10.1111/j.1601-183X.2004.00093.x.

**Britt JP, Benaliouad F, McDevitt RA, Stuber GD, Wise RA, Bonci A.** Synaptic and behavioral profile of multiple glutamatergic inputs to the nucleus accumbens. *Neuron* 76: 790–803, 2012. doi:10.1016/j.neuron.2012.09.040.

**Calabresi P, Mercuri N, Stanzione P, Stefani A, Bernardi G.** Intracellular studies on the dopamine-induced firing inhibition of neostriatal neurons in vitro: evidence for D1 receptor involvement. *Neuroscience* 20: 757–771, 1987. doi:10.1016/0306-4522(87)90239-9.

**Cao J, Dorris DM, Meitzen J.** Neonatal masculinization blocks increased excitatory synaptic input in female rat nucleus accumbens core. *Endocrinology* 157: 3181–3196, 2016. doi:10.1210/en.2016-1160.

**Carter CS, DeVries AC, Getz LL.** Physiological substrates of mammalian monogamy: the prairie vole model. *Neurosci Biobehav Rev* 19: 303–314, 1995. doi:10.1016/0149-7634(94)00070-H.

**Carter CS, Getz LL.** Monogamy and the prairie vole. *Sci Am* 268: 100–106, 1993. doi:10.1038/scientificamerican0693-100.

**Cepeda C, André VM, Yamazaki I, Wu N, Kleiman-Weiner M, Levine MS.** Differential electrophysiological properties of dopamine D1 and D2 receptor-containing striatal medium-sized spiny neurons. *Eur J Neurosci* 27: 671–682, 2008. doi:10.1111/j.1460-9568.2008.06038.x.

**Cepeda C, Walsh JP, Peacock W, Buchwald NA, Levine MS.** Neurophysiological, pharmacological and morphological properties of human caudate neurons recorded in vitro. *Neuroscience* 59: 89–103, 1994. doi:10.1016/0306-4522(94)90101-5.

**Dorris DM, Cao J, Willett JA, Hauser CA, Meitzen J.** Intrinsic excitability varies by sex in prepubertal striatal medium spiny neurons. *J Neurophysiol* 113: 720–729, 2015. doi:10.1152/jn.00687.2014.

**Dorris DM, Hauser CA, Minnehan CE, Meitzen J.** An aerator for brain slice experiments in individual cell culture plate wells. *J Neurosci Methods* 238: 1–10, 2014. doi:10.1016/j.jneumeth.2014.09.017.

**Farries MA, Meitzen J, Perkel DJ.** Electrophysiological properties of neurons in the basal ganglia of the domestic chick: conservation and divergence in the evolution of the avian basal ganglia. *J Neurophysiol* 94: 454–467, 2005. doi:10.1152/jn.00539.2004.

**Farries MA, Perkel DJ.** Electrophysiological properties of avian basal ganglia neurons recorded in vitro. *J Neurophysiol* 84: 2502–2513, 2000. doi:10.1152/jn.2000.84.5.2502.

**Farries MA, Perkel DJ.** A telencephalic nucleus essential for song learning contains neurons with physiological characteristics of both striatum and globus pallidus. *J Neurosci* 22: 3776–3787, 2002.

**Galarraga E, Bargas J, Sierra A, Aceves J.** The role of calcium in the repetitive firing of neostriatal neurons. *Exp Brain Res* 75: 157–168, 1989. doi:10.1007/BF00248539.

**Gertler TS, Chan CS, Surmeier DJ.** Dichotomous anatomical properties of adult striatal medium spiny neurons. *J Neurosci* 28: 10814–10824, 2008. doi:10.1523/JNEUROSCI.2660-08.2008.

**Getz LL, Carter CS.** Prairie-vole partnerships. *Am Sci* 84: 56–62, 1996.

**Getz LL, McGuire B, Pizzuto T, Hofmann JE, Frase B.** Social organization of the prairie vole (*Microtus ochrogaster*). *J Mammal* 74: 44–58, 1993. doi:10.2307/1381904.

**Grillner S, Hellgren J, Ménard A, Saitoh K, Wikström MA.** Mechanisms for selection of basic motor programs—roles for the striatum and pallidum. *Trends Neurosci* 28: 364–370, 2005. doi:10.1016/j.tins.2005.05.004.

**Groenewegen HJ, Wright CI, Beijer AV, Voorn P.** Convergence and segregation of ventral striatal inputs and outputs. *Ann NY Acad Sci* 877: 49–63, 1999. doi:10.1111/j.1749-6632.1999.tb09260.x.

**Gruber AJ, O'Donnell P.** Bursting activation of prefrontal cortex drives sustained up states in nucleus accumbens spiny neurons in vivo. *Synapse* 63: 173–180, 2009. doi:10.1002/syn.20593.

**Hammock EA, Young LJ.** Microsatellite instability generates diversity in brain and sociobehavioral traits. *Science* 308: 1630–1634, 2005. doi:10.1126/science.1111427.

**Hammock EA, Young LJ.** Oxytocin, vasopressin and pair bonding: implications for autism. *Philos Trans R Soc Lond B Biol Sci* 361: 2187–2198, 2006. doi:10.1098/rstb.2006.1939.

**Heimer L, Zahm DS, Churchill L, Kalivas PW, Wohltmann C.** Specificity in the projection patterns of accumbal core and shell in the rat. *Neuroscience* 41: 89–125, 1991. doi:10.1016/0306-4522(91)90202-Y.

**Ikemoto S, Witkin BM.** Locomotor inhibition induced by procaine injections into the nucleus accumbens core, but not the medial ventral striatum: implication for cocaine-induced locomotion. *Synapse* 47: 117–122, 2003. doi:10.1002/syn.10151.

**Insel TR, Shapiro LE.** Oxytocin receptor distribution reflects social organization in monogamous and polygamous voles. *Proc Natl Acad Sci USA* 89: 5981–5985, 1992. doi:10.1073/pnas.89.13.5981.

**Jeanblanc J, Hoeltzel A, Louilot A.** Dissociation in the involvement of dopaminergic neurons innervating the core and shell subregions of the nucleus accumbens in latent inhibition and affective perception. *Neuroscience* 111: 315–323, 2002. doi:10.1016/S0306-4522(02)00019-2.

**Kelley AE.** Ventral striatal control of appetitive motivation: role in ingestive behavior and reward-related learning. *Neurosci Biobehav Rev* 27: 765–776, 2004. doi:10.1016/j.neubiorev.2003.11.015.

**Kelly PH, Roberts DC.** Effects of amphetamine and apomorphine on locomotor activity after 6-OHDA and electrolytic lesions of the nucleus accumbens septi. *Pharmacol Biochem Behav* 19: 137–143, 1983. doi:10.1016/0091-3057(83)90322-2.

**Kimura M.** Behaviorally contingent property of movement-related activity of the primate putamen. *J Neurophysiol* 63: 1277–1296, 1990. doi:10.1152/jn.1990.63.6.1277.

**Kimura M, Kato M, Shimazaki H.** Physiological properties of projection neurons in the monkey striatum to the globus pallidus. *Exp Brain Res* 82: 672–676, 1990. doi:10.1007/BF00228811.

**Kleiman DG.** Monogamy in mammals. *Q Rev Biol* 52: 39–69, 1977. doi:10.1086/409721.

**Lim MM, Wang Z, Olazábal DE, Ren X, Terwilliger EF, Young LJ.** Enhanced partner preference in a promiscuous species by manipulating the expression of a single gene. *Nature* 429: 754–757, 2004. doi:10.1038/nature02539.

**Ma YY, Cepeda C, Chatta P, Franklin L, Evans CJ, Levine MS.** Regional and cell-type-specific effects of DAMGO on striatal D1 and D2 dopamine receptor-expressing medium-sized spiny neurons. *ASN Neuro* 4: e00077, 2012. doi:10.1042/AN20110063.

**McGraw LA, Young LJ.** The prairie vole: an emerging model organism for understanding the social brain. *Trends Neurosci* 33: 103–109, 2010. doi:10.1016/j.tins.2009.11.006.

**McGuire B, Getz LL.** Alternative male reproductive tactics in a natural population of prairie voles *Microtus ochrogaster*. *Acta Theriol (Warsz)* 55: 261–270, 2010. doi:10.4098/j.at.0001-7051.077.2009.

**Meisel RL, Mullins AJ.** Sexual experience in female rodents: cellular mechanisms and functional consequences. *Brain Res* 1126: 56–65, 2006. doi:10.1016/j.brainres.2006.08.050.

**Meitzen J, Weaver AL, Brenowitz EA, Perkel DJ.** Plastic and stable electrophysiological properties of adult avian forebrain song-control neurons across changing breeding conditions. *J Neurosci* 29: 6558–6567, 2009. doi:10.1523/JNEUROSCI.5571-08.2009.

**Meredith GE, Baldo BA, Andrezjewski ME, Kelley AE.** The structural basis for mapping behavior onto the ventral striatum and its subdivisions. *Brain Struct Funct* 213: 17–27, 2008. doi:10.1007/s00429-008-0175-3.

**Mu P, Moyer JT, Ishikawa M, Zhang Y, Panksepp J, Sorg BA, Schlüter OM, Dong Y.** Exposure to cocaine dynamically regulates the intrinsic membrane excitability of nucleus accumbens neurons. *J Neurosci* 30: 3689–3699, 2010. doi:10.1523/JNEUROSCI.4063-09.2010.

**Nisenbaum ES, Xu ZC, Wilson CJ.** Contribution of a slowly inactivating potassium current to the transition to firing of neostriatal spiny projection neurons. *J Neurophysiol* 71: 1174–1189, 1994. doi:10.1152/jn.1994.71.3.1174.

**Numan M.** Motivational systems and the neural circuitry of maternal behavior in the rat. *Dev Psychobiol* 49: 12–21, 2007. doi:10.1002/dev.20198.

**O'Donnell P, Grace AA.** Physiological and morphological properties of accumbens core and shell neurons recorded in vitro. *Synapse* 13: 135–160, 1993. doi:10.1002/syn.890130206.

**Okhovat M, Berrio A, Wallace G, Ophir AG, Phelps SM.** Sexual fidelity trade-offs promote regulatory variation in the prairie vole brain. *Science* 350: 1371–1374, 2015. doi:10.1126/science.aac5791.

**Olazábal DE, Young LJ.** Oxytocin receptors in the nucleus accumbens facilitate "spontaneous" maternal behavior in adult female prairie voles. *Neuroscience* 141: 559–568, 2006a. doi:10.1016/j.neuroscience.2006.04.017.

**Olazábal DE, Young LJ.** Species and individual differences in juvenile female alloparental care are associated with oxytocin receptor density in the striatum and the lateral septum. *Horm Behav* 49: 681–687, 2006b. doi:10.1016/j.yhbeh.2005.12.010.

**Ophir AG, Wolff JO, Phelps SM.** Variation in neural V1aR predicts sexual fidelity and space use among male prairie voles in semi-natural settings. *Proc Natl Acad Sci USA* 105: 1249–1254, 2008. doi:10.1073/pnas.0709116105.

**Opris I, Lebedev M, Nelson RJ.** Motor planning under unpredictable reward: modulations of movement vigor and primate striatum activity. *Front Neurosci* 5: 61, 2011. doi:10.3389/fnins.2011.00061.

**Parkinson JA, Olmstead MC, Burns LH, Robbins TW, Everitt BJ.** Dissociation in effects of lesions of the nucleus accumbens core and shell on appetitive Pavlovian approach behavior and the potentiation of conditioned reinforcement and locomotor activity by D-amphetamine. *J Neurosci* 19: 2401–2411, 1999.

**Perkeybile AM, Bales KL.** Intergenerational transmission of sociality: the role of parents in shaping social behavior in monogamous and non-monogamous species. *J Exp Biol* 220: 114–123, 2017. doi:10.1242/jeb.142182.

**Perkeybile AM, Griffin LL, Bales KL.** Natural variation in early parental care correlates with social behaviors in adolescent prairie voles (*Microtus ochrogaster*). *Front Behav Neurosci* 7: 21, 2013. doi:10.3389/fnbeh.2013.00021.

**Pineda JC, Galarraga E, Bargas J, Cristancho M, Aceves J.** Charybdotoxin and apamin sensitivity of the calcium-dependent repolarization and the afterhyperpolarization in neostriatal neurons. *J Neurophysiol* 68: 287–294, 1992. doi:10.1152/jn.1992.68.1.287.

**Pitchers KK, Frohmader KS, Vialou V, Mouzon E, Nestler EJ, Lehman MN, Coolen LM.** ΔFosB in the nucleus accumbens is critical for reinforcing effects of sexual reward. *Genes Brain Behav* 9: 831–840, 2010. doi:10.1111/j.1601-183X.2010.00621.x.

**Pitchers KK, Schmid S, Di Sebastiano AR, Wang X, Laviolette SR, Lehman MN, Coolen LM.** Natural reward experience alters AMPA and NMDA receptor distribution and function in the nucleus accumbens. *PLoS One* 7: e34700, 2012. doi:10.1371/journal.pone.0034700.

**Planert H, Berger TK, Silberberg G.** Membrane properties of striatal direct and indirect pathway neurons in mouse and rat slices and their modulation by dopamine. *PLoS One* 8: e57054, 2013. doi:10.1371/journal.pone.0057054.

**Ross HE, Cole CD, Smith Y, Neumann ID, Landgraf R, Murphy AZ, Young LJ.** Characterization of the oxytocin system regulating affiliative behavior in female prairie voles. *Neuroscience* 162: 892–903, 2009. doi:10.1016/j.neuroscience.2009.05.055.

**Salgado S, Kaplitt MG.** The nucleus accumbens: a comprehensive review. *Stereotact Funct Neurosurg* 93: 75–93, 2015. doi:10.1159/000368279.

**Slob AK, de Klerk LW, Brand T.** Homosexual and heterosexual partner preference in ovariectomized female rats: effects of testosterone, estradiol and mating experience. *Physiol Behav* 41: 571–576, 1987. doi:10.1016/0031-9384(87)90313-1.

**Smith RJ, Lobo MK, Spencer S, Kalivas PW.** Cocaine-induced adaptations in D1 and D2 accumbens projection neurons (a dichotomy not necessarily synonymous with direct and indirect pathways). *Curr Opin Neurobiol* 23: 546–552, 2013. doi:10.1016/j.conb.2013.01.026.

**Staffend NA, Hedges VL, Chemel BR, Watts VJ, Meisel RL.** Cell-type specific increases in female hamster nucleus accumbens spine density following female sexual experience. *Brain Struct Funct* 219: 2071–2081, 2014. doi:10.1007/s00429-013-0624-5.

**Tan CL, Plotkin JL, Venø MT, von Schimmelmann M, Feinberg P, Mann S, Handler A, Kjems J, Surmeier DJ, O'Carroll D, Greengard P, Schaefer A.** MicroRNA-128 governs neuronal excitability and motor behavior in mice. *Science* 342: 1254–1258, 2013. doi:10.1126/science.1244193.

**Vucetic Z, Reyes TM.** Central dopaminergic circuitry controlling food intake and reward: implications for the regulation of obesity. *Wiley Interdiscip Rev Syst Biol Med* 2: 577–593, 2010. doi:10.1002/wsbm.77.

**Willett JA, Will T, Hauser CA, Dorris DM, Cao J, Meitzen J.** No evidence for sex differences in the electrophysiological properties and excitatory synaptic input onto nucleus accumbens shell medium spiny neurons. *eNeuro* 3: ENEURO.0147-15.2016, 2016. doi:10.1523/ENEURO.0147-15.2016.

**Williams JR, Catania KC, Carter CS.** Development of partner preferences in female prairie voles (*Microtus ochrogaster*): the role of social and sexual experience. *Horm Behav* 26: 339–349, 1992. doi:10.1016/0018-506X(92)90004-F.

**Wilson CJ.** Predicting the response of striatal spiny neurons to sinusoidal input. *J Neurophysiol* 118: 855–873, 2017. doi:10.1152/jn.00143.2017.

**Wilson CJ, Groves PM.** Spontaneous firing patterns of identified spiny neurons in the rat neostriatum. *Brain Res* 220: 67–80, 1981. doi:10.1016/0006-8993(81)90211-0.

**Wissman AM, McCollum AF, Huang GZ, Nikrodhanond AA, Woolley CS.** Sex differences and effects of cocaine on excitatory synapses in the nucleus accumbens. *Neuropharmacology* 61: 217–227, 2011. doi:10.1016/j.neuropharm.2011.04.002.

**Wolf ME.** The Bermuda Triangle of cocaine-induced neuroadaptations. *Trends Neurosci* 33: 391–398, 2010. doi:10.1016/j.tins.2010.06.003.

**Yager LM, Garcia AF, Wunsch AM, Ferguson SM.** The ins and outs of the striatum: role in drug addiction. *Neuroscience* 301: 529–541, 2015. doi:10.1016/j.neuroscience.2015.06.033.

**Yoshida M, Yokoo H, Mizoguchi K, Kawahara H, Tsuda A, Nishikawa T, Tanaka M.** Eating and drinking cause increased dopamine release in the nucleus accumbens and ventral tegmental area in the rat: measurement by in vivo microdialysis. *Neurosci Lett* 139: 73–76, 1992. doi:10.1016/0304-3940(92)90861-Z.

**Young KA, Gobrogge KL, Liu Y, Wang Z.** The neurobiology of pair bonding: insights from a socially monogamous rodent. *Front Neuroendocrinol* 32: 53–69, 2011. doi:10.1016/j.yfrne.2010.07.006.

**Young LJ, Wang Z.** The neurobiology of pair bonding. *Nat Neurosci* 7: 1048–1054, 2004. doi:10.1038/nn1327.

**Zahm DS, Brog JS.** On the significance of subterritories in the "accumbens" part of the rat ventral striatum. *Neuroscience* 50: 751–767, 1992. doi:10.1016/0306-4522(92)90202-D.

**Zahm DS, Heimer L.** Specificity in the efferent projections of the nucleus accumbens in the rat: comparison of the rostral pole projection patterns with those of the core and shell. *J Comp Neurol* 327: 220–232, 1993. doi:10.1002/cne.903270205.